New Journal of Physics
The open–access journal for physics

Search for orbitons in $LaMnO_3$, $YTiO_3$ and $KCuF_3$ using high-resolution inelastic x-ray scattering

Yoshikazu Tanaka[1,6], A Q R Baron[2], Young-June Kim[3], K J Thomas[3], J P Hill[3], Z Honda[4], F Iga[5], S Tsutsui[2], D Ishikawa[1] and C S Nelson[3]

[1] SPring-8/RIKEN, Sayo, Hyogo 679-5148, Japan
[2] SPring-8/JASRI, Sayo, Hyogo 679-5198, Japan
[3] Department of Physics, Brookhaven National Laboratory, Upton, NY 11973, USA
[4] Saitama University, Saitama 338-8570, Japan
[5] Graduate School of Advanced Science of Matter, Hiroshima University, Higashi-Hiroshima 739-8530, Japan
E-mail: ytanaka@riken.jp

New Journal of Physics **6** (2004) 161
Received 10 August 2004
Published 5 November 2004
Online at http://www.njp.org/
doi:10.1088/1367-2630/6/1/161

Abstract. Orbital excitations have been sought in three systems, $LaMnO_3$, $KCuF_3$ and $YTiO_3$, using high-resolution inelastic x-ray scattering, with an energy resolution of 6 meV. Motivated by the recent Raman scattering result of Saitoh *et al* (2001 *Nature* **410** 180), we measured the energy transfer spectra of $LaMnO_3$ in the energy range up to 200 meV. We did not find any signal above background that could be associated with orbiton excitations. Since significant interaction between the spin and orbital degrees of freedom is expected in $KCuF_3$ and $YTiO_3$, energy spectra were measured above and below the respective magnetic ordering temperature. We were not able to detect any change in the excitation spectra due to the magnetic ordering temperature of these materials. We discuss the implications of the experimental findings and estimate an upper bound on the orbiton x-ray cross-section.

[6] Author to whom any correspondence should be addressed.

PII: S1367-2630(04)84752-9

Contents

1. Introduction

In order to fully model the physics in many correlated electron materials, such as the colossal magnetoresistive manganites, the orbital degree of freedom must be considered on equal footing with the spin, charge and electron–lattice coupling. The occupancy of a particular valence orbital on an atomic site has an important role in determining the magnetic coupling—ferromagnetic or antiferromagnetic—between neighbouring ions. In fact, orbital ordering, in which the orbital occupancy has a definite orientation from site to site, is often viewed as a precursor to magnetic ordering [1]–[3], while short-range orbital correlations may be fundamental to understanding the large magnetoresistance found in manganites [4]. From a theoretical standpoint, there is also considerable interest in possible liquid-like behaviour in some orbitally degenerate systems [5]. This broad interest in orbital physics is encouraging a number of experiments in which one tries to 'see' the orbital order and measure its associated excitations.

The canonical example of an orbitally ordered system is the perovskite manganite $LaMnO_3$. $LaMnO_3$ is an antiferromagnetic insulator, consisting of trivalent Mn ions with four electrons in the 3d orbitals, which are split by the crystal field potential from the surrounding oxygen ions. The Mn^{3+} ions are found in the high-spin state with the electronic configuration $(t_{2g})^3(e_g)^1$, with one electron occupying the doubly degenerate e_g orbitals [1]–[3]. Below ∼780 K, the orbital degeneracy is spontaneously broken by a cooperative Jahn–Teller (JT) lattice distortion and the orbital orders. The orbital order is described as $d_{3x^2-r^2}$ and $d_{3y^2-r^2}$ orbitals, which are alternately occupied in the *ab* plane. Both x-ray and neutron diffraction experiments can indirectly probe the orbital ordering via the cooperative JT distortion [6, 7]. Recently, orbital ordering in related half-doped manganites has been directly detected by soft x-ray resonant scattering at the Mn L-edges [8]–[10].

The ordering of orbitals implies the existence of collective excitations, similar to spin-wave excitations in a spin-ordered phase. In a simple picture, in which the e_g electrons are strictly localized, the lowest energy electronic excitation corresponds to the localized excitation of order E_{JT}, the JT energy splitting of the e_g orbitals. If we introduce non-zero coupling between orbitals on adjacent Mn sites, collective excitations of the orbital degree of freedom, or *orbitons* are expected [11]. However, the orbital degree of freedom lacks continuous rotational symmetry and, as a result, the orbiton spectrum must have a gap.

Two physically distinct mechanisms have been proposed to describe the energy scale of the orbitons. One is the electron–electron coupling, which splits the states via the superexchange interaction between nearest neighbouring Mn ions. This model predicts relatively small energies, ∼0.1–0.2 eV, for the orbitons [12]. On the other hand, alternative approaches lead to a typical energy scale ∼1 eV [13]. In complex materials, such as manganites, both mechanisms may be relevant [14].

Clearly, measuring the energy and dispersion of these orbitons would reveal much about the underlying mechanism for the orbital order, as well as the relevant energy scales. In a Raman scattering experiment on $LaMnO_3$, Saitoh *et al* [12] assigned the weak features observed between 125 and 160 meV to orbitons based on their calculations using the superexchange model (i.e. no coupling to the lattice). They showed that these features disappear at the same temperature as phonon modes associated with the JT distortion. However, there is considerable debate about this interpretation. Grüninger *et al* suggested that the 160 meV peak in the spectra [12, 15] could be due to multiphonon effects because such signals have been observed in a similar energy range in the optical conductivity spectra [15, 16]. Moreover, two independent groups recently concluded that the observed peaks around 160 meV result from phonon, and not orbiton, excitations [17, 18]. Thus interpretation of the peaks observed by Saitoh *et al* [12] remains controversial. Clearly, it would be of value to study this question with alternative techniques to help resolve this issue.

Inelastic x-ray scattering (IXS) has become an important technique to study collective excitations in condensed matter systems, complementing inelastic neutron scattering (INS). The IXS cross-section is directly proportional to the dynamic structure factor, which is a probe-independent, solid-state property of the system. Therefore, the interpretation of IXS data is straightforward and a well-developed scattering theory can be applied to understand the cross-section. However, there is a fundamental difference between the IXS and INS cross-sections. Unlike neutrons, which interact with the atomic nuclei, x-rays interact with the electrons. Thus, IXS is sensitive to both electronic excitations, through the valence electrons, and phonon excitations, through the core electrons. In principle, IXS should be sensitive to orbital excitations, although phonon processes may dominate the IXS because there are many more core electrons than valence electrons.

In this paper, we discuss a series of experiments in which we used high-resolution IXS to search for orbital excitations in three prototypical orbitally ordered systems, $LaMnO_3$, $KCuF_3$ and $YTiO_3$. IXS has the advantage compared to Raman scattering that the orbital excitation, if found, can be measured over the entire Brillouin zone. Since the phonon contribution is expected to dominate the IXS signal, we rely heavily on the assumption that the orbital excitations are strongly temperature dependent around the magnetic ordering temperature in $YTiO_3$ and $KCuF_3$, or that the orbiton energy scale is well separated from the phonon energy scale as suggested by the Raman scattering study of $LaMnO_3$.

As shown below, we do not observe scattering which could be ascribed to an orbital excitation in any of the materials studied. We will present data showing these results and discuss implications of our experimental findings.

2. Experimental setup

High-resolution IXS experiments have been carried out at the beamline BL35XU at SPring-8 in Harima, Japan. The spectrometer is similar to a neutron triple-axis spectrometer, and consists of a backscattering monochromator and a multiple analyser setup [19]. The Si (8 8 8) backscattering

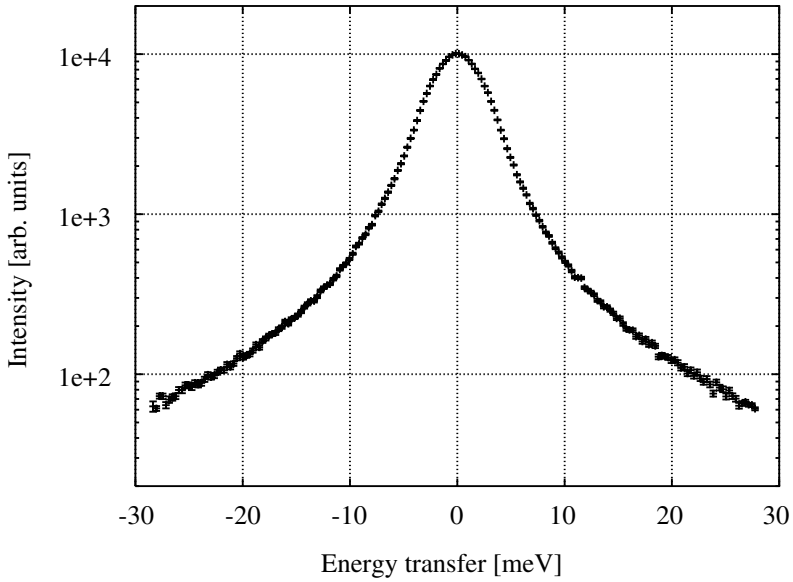

Figure 1. A resolution spectrum measured with a 5 mm thick PMMA.

monochromator provides an incident beam with a narrow energy bandwidth of about 4 meV at 15.816 keV. The beam was focused to a $0.13 \times 0.1\,\mathrm{mm}^2$ spot at the sample position by a cylindrical mirror with a flux of about 3×10^{10} photons s^{-1} at the maximum current (100 mA) of the SPring-8. We used four spherical Si (8 8 8) analyser crystals, placed with 0.78° spacing on the 10 m-long 2θ arm, which focus the scattered beam to four independent CdZnTe detectors. This allows us to measure energy spectra at four different momentum transfer (**Q**) positions simultaneously. At each **Q** position, the incident energy (E_i) is scanned by varying the temperature of the monochromator crystal, utilizing the temperature-dependent change of the lattice spacing of silicon. The final energy, E_f, is held fixed by carefully maintaining the analyser crystals at a constant temperature. The energy spectra are normalized by the intensity of the monitor located before the sample. Single crystal samples were mounted in a closed cycle ^{4}He refrigerator and cooled down to low temperatures. Due to the low scattering intensity, each energy spectrum was measured for 12–18 h by repeating scans for a total of 10–15 minutes per point.

The resolution function of the spectrometer for each analyser crystal was measured with a 5 mm thick PMMA plate. The total energy resolution is about 6 meV, full-width-at-half-maximum (FWHM). The momentum resolution is determined by the full diameter of each analyser crystal, which is 95 mm and gives a momentum resolution of about 0.07 $\mathrm{Å}^{-1}$ (FWHM). Figure 1 shows the resolution function for analyser crystal #1 located at the lowest 2θ angle among the four. The FWHM is 5.9 meV. Unlike INS, the IXS experiment has the advantage that the resolution is independent of **Q**, but has the disadvantage that the resolution function has a long Lorentzian tail. This means that lower energy excitations or quasi-elastic signal—from surface roughness, defects, etc—contributes strongly to the background.

3. Experimental results

We chose to study three materials, which exhibit very different orbital/magnetic ordering behaviour. All three materials have a perovskite-like structure and show orbital ordering

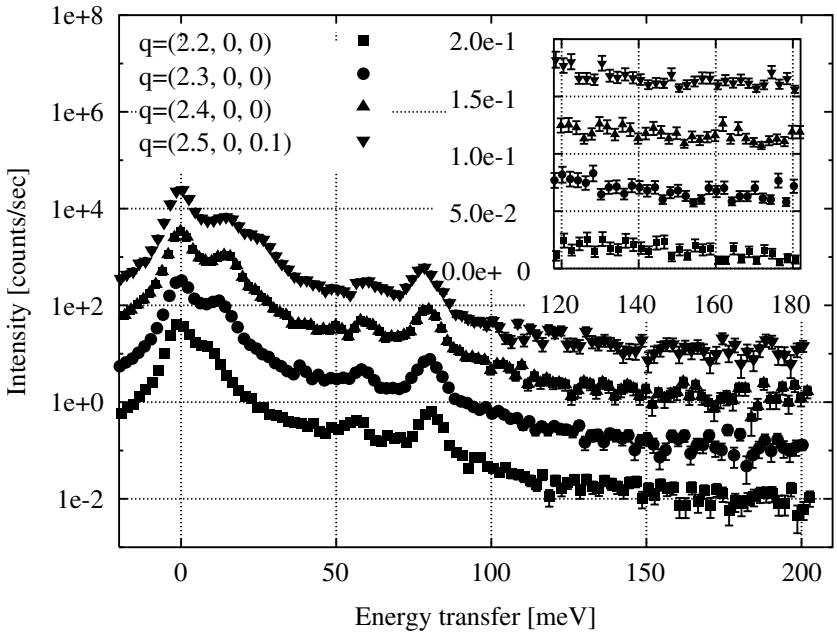

Figure 2. Energy spectra of IXS of $LaMnO_3$ measured at $q = (2.2, 0, 0)$, $(2.3, 0, 0)$, $(2.4, 0, 0)$ and $(2.5, 0, 0.1)$ at 35 K. The intensity is shown on a logarithmic scale in units of counts s^{-1} (cps). Each spectrum is offset vertically for clarity by multiplying a constant (1, 10, 100 and 1000 from bottom to top). Inset: energy spectra on a linear scale in the range 120–180 meV. Each spectrum is offset vertically by 0.05 for clarity.

associated with cooperative JT distortion at very high temperatures. However, $LaMnO_3$ (d^4) and $KCuF_3$ (d^9) have degenerate e_g orbitals (an electron orbital for $LaMnO_3$ and a hole orbital for $KCuF_3$), while $YTiO_3$ (d^1) has degenerate t_{2g} orbitals. Both $LaMnO_3$ and $KCuF_3$ have so-called *A*-type antiferromagnetic ordering below 140 and 38 K, respectively, while $YTiO_3$ orders ferromagnetically below 30 K.

3.1. $LaMnO_3$

The room-temperature crystal structure of $LaMnO_3$ belongs to the orthorhombic space group Pbnm (#62) with lattice constants $a = 5.5367$ Å, $b = 5.7473$ Å and $c = 7.6929$ Å [7]. The system goes into the *A*-type antiferromagnetic phase below $T_N = 140$ K [20]. A single crystal, grown by the floating zone method, was cut into a few mm^3 in size. The sample had two flat surfaces: one was normal to the *a*-axis and the other was normal to the *c*-axis. The measurements were carried out in two geometries: (i) **Q** was parallel to the *a*-axis and the *c*-axis was in the scattering plane. In this geometry, the dispersion along Γ–M, (0 0 0)–(π π 0) in the tetragonal Brillouin zone, is scanned. (ii) **Q** was parallel to the *c*-axis and the *a*-axis was in the scattering plane. In this geometry, the dispersion along Γ–Z, (0 0 0)–(0 0 π), is scanned. It is noted that the longitudinal (transverse) phonon modes are active (inactive) in both geometries. We chose zones of reciprocal space where the orbiton was expected to have a relatively large structure factor based on a calculation by Ishihara [21].

In figure 2, we plot the inelastic scattering intensity, on a logarithmic scale, as a function of energy transfer at various **Q** positions along the *a*-axis (Γ–M) at 35 K (below T_N). These

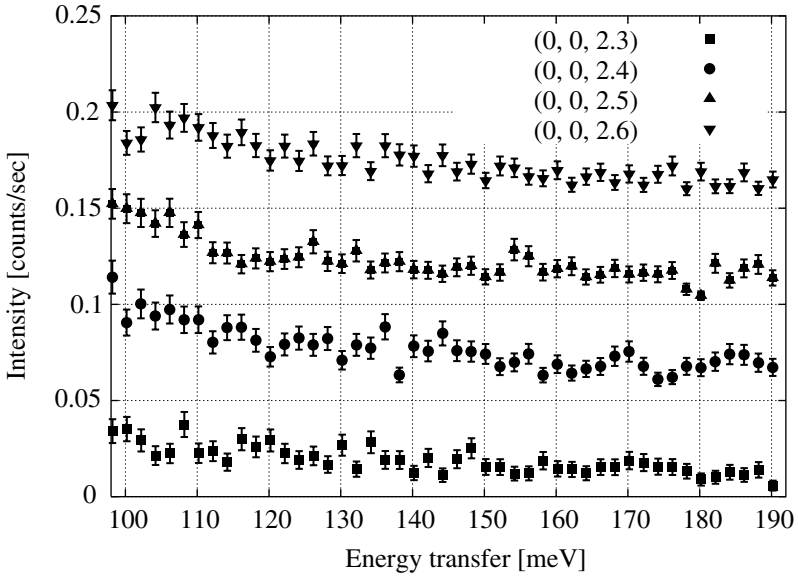

Figure 3. Energy spectra of IXS of $LaMnO_3$ measured at $q = (0, 0, 2.3)$, $(0, 0, 2.4)$, $(0, 0, 2.5)$ and $(0, 0, 2.6)$ at 44 K. Each spectrum is offset vertically by 0.05 for clarity.

four **Q** positions correspond to four different analysers, and they were thus obtained at the same time. Several phonon peaks are observed in each spectrum. An acoustic mode is observed as a peak below 20 meV and exhibits large dispersion. The peaks around 55 and 80 meV, which were observed in the Raman scattering data obtained by Martín-Carrón *et al* [22], have small dispersions. They assigned these peaks to the JT mode and the breathing mode, respectively. Guided by the earlier Raman scattering data obtained by Saitoh *et al* [12], we focus our attention on the energy range 120–180 meV. In the inset to figure 2, the energy spectra in this energy range are shown on a linear scale. The Raman scattering data have three peaks in this energy range [12], which were attributed to orbiton modes at the Brillouin zone centre. However, to within our statistical error, we observed no peaks above background.

In the second geometry, the energy spectra along the c-axis (Γ–Z) were measured at 44 K (again below T_N). In figure 3, we plot the scattered intensity in this geometry for the energy range 110–190 meV on a linear scale. Within experimental uncertainties, we again observe no peaks. Since the orbital ordering temperature of $LaMnO_3$ is rather high (∼780 K), we were not able to measure the temperature dependence of the inelastic spectra across the orbital ordering temperature.

3.2. $KCuF_3$

The crystal structure of $KCuF_3$ is composed of distorted CuF_6 octahedra due to a cooperative JT distortion at a very high temperature. The accompanying *hole* orbital ordering pattern is that of alternating $d_{z^2-x^2}$ and $d_{z^2-y^2}$ orbitals in the *ab*-plane. There are two polytypes of the orbital ordering pattern depending on the stacking of these *ab*-planes [23]: *a*-type with a space group I4/mcm (#140) and lattice constants $a = b = 5.8569$ and $c = 7.8487$ Å and *d*-type with a space group P/4mbm(#127). These two types of structures exhibit different magnetic ordering temperatures [24], with $T_N \sim 38$ K and $T_N \sim 22$ K for the *a*-type and the *d*-type, respectively. The

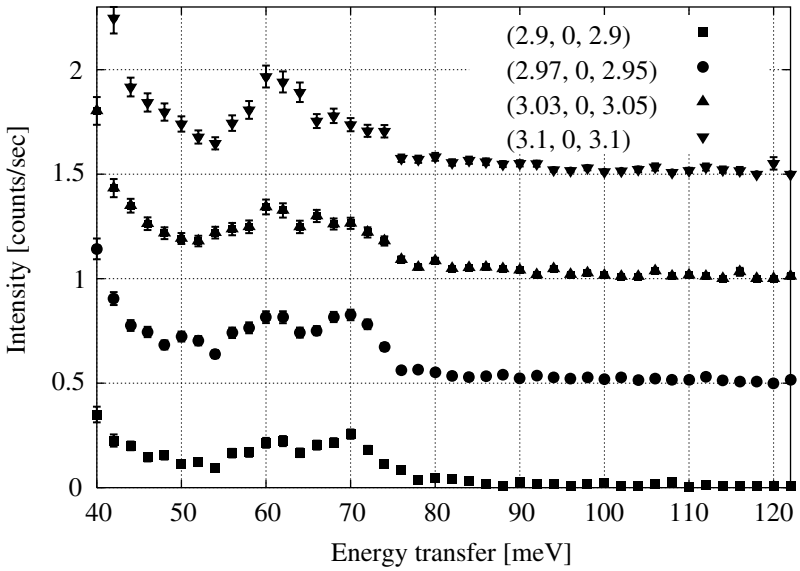

Figure 4. Energy spectra of $KCuF_3$ measured at $q = (2.9, 0, 2.9)$, $(2.97, 0, 2.95)$, $(3.03, 0, 3.05)$ and $(3.1, 0, 3.1)$ at 15 K. The intensity is shown in a linear scale. Each spectrum is offset vertically by 0.5 for clarity.

sample used in our experiment was predominantly *a*-type. In their pioneering work, Kugel and Khomskii [3] proposed a superexchange-driven orbital-ordering picture, which is consistent with the experimentally observed orbital-order structure in $KCuF_3$. In addition, large wavefunction overlap exists only along the *c*-direction for this orbital-order structure, which in turn should result in a strong one-dimensional magnetism along the *c*-direction. This has been seen experimentally with neutron scattering techniques [25, 26].

In a recent resonant x-ray scattering experiment, Paolasini *et al* [27] were able to study the temperature dependence of the superlattice reflections arising from magnetic and orbital order, respectively. Surprisingly, a dramatic increase of the orbital order parameter was observed at temperatures below the magnetic ordering temperature, suggesting a strong coupling between the orbital and spin degrees of freedom. Additional motivation for our experiment came from a theoretical study of the spin and orbital excitation spectra of a $KCuF_3$-like system: Oles *et al* [28] considered a spin–orbital model for a d^9 system in a perovskite structure and calculated the excitation spectra explicitly. However, since the predicted energy scale for orbital-wave excitations in $KCuF_3$ is of order $\sim 4J$ ($J \sim 15$ meV [26]) in this material, it is essential to be able to distinguish orbitons from phonons. Since there exists a strong spin–orbital interaction in $KCuF_3$, one would expect strong modification of the orbiton excitation spectra when the system goes through the magnetic ordering transition—in particular, in light of the apparent large change in the orbital order parameter at this temperature [27]. Therefore, we have studied the temperature dependence of the excitation spectra of $KCuF_3$ above and below the magnetic ordering temperature, in an attempt to detect change in the spin–orbital excitation spectra due to magnetic ordering.

We have measured the IXS intensity as a function of energy transfer at the orbital ordering wavevector (3 0 3). A large single crystal, which was used in earlier neutron scattering studies [26], was used in our measurement. In figure 4, the energy scans taken at $T = 15$ K are shown for four momentum transfers. As expected, strong contributions from phonons dominate most of the

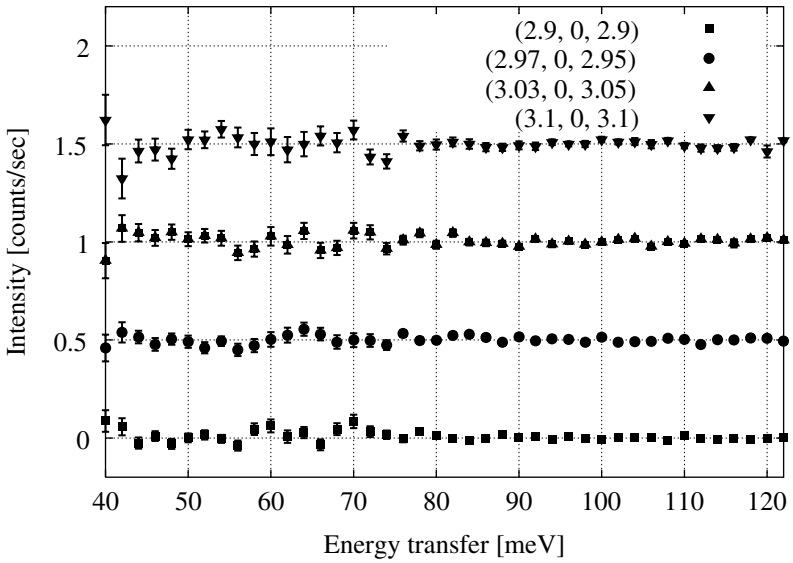

Figure 5. Difference in the intensity measured at 45 and 15 K for $KCuF_3$. Each spectrum is offset vertically by 0.5 for clarity.

spectra up to ∼80 meV. The phonon positions are consistent with a Raman scattering study [29] and also with shell-model calculations. In figure 5, we plot the difference between the spectra at $T = 45$ and 15 K, which correspond to temperatures above and below T_N, respectively. We could not observe any difference between the two temperatures, within experimental uncertainties. We have also observed a similar temperature-independent behaviour of x-ray spectra at the zone boundary position at (1.5 0 1.5). Based on our limited data, we conclude that orbiton excitation was not observed in the energy range up to ∼160 meV in $KCuF_3$, in our IXS study.

3.3. $YTiO_3$

$YTiO_3$ is a ferromagnetic insulator with $T_C \sim 30$ K. The space group is Pbnm (#62), i.e., the same as that for $LaMnO_3$, and the lattice constants are $a = 5.3584$ Å, $b = 5.6956$ Å and $c = 7.6371$ Å at room temperature [30, 31]. The electronic configuration of the Ti^{3+} ions is $(t_{2g})^1$, and the orbital degeneracy is lifted by a JT distortion. The orbitally ordered structure has been confirmed by several experimental methods [32]–[34].

In t_{2g} orbital systems, the electron–phonon coupling is believed to be weaker because of the higher degeneracy compared to the e_g systems, and the fact that the t_{2g} orbitals point away from the oxygen ions, greatly weakening their interaction. One may therefore expect a larger interaction between the orbital and spin dynamics because the orbital ordering is expected to be driven by the superexchange interactions. Theoretical studies of the orbiton spectrum in $YTiO_3$ have been carried out by Khaliullin and Okamoto [35] and also by Ishihara [36]. They calculated the excitation spectrum of the orbital-ordered state in the presence of ferromagnetic spin ordering, and predicted the existence of orbitons in the energy range up to ∼100 meV, although the detailed dispersion relation looks different in the two calculations.[7]

[7] The orbiton spectrum of $YTiO_3$ calculated by Khaliullin and Okamoto [35] has a gap of 0.57 and a bandwidth of ∼0.5 in units of $r_1 J_{SE}$, which is estimated to be around 60–80 meV. The orbiton spectrum predicted by Ishihara [36] contains several modes ranging from 1 to 4 in units of J_0, which is estimated to be smaller than 33 meV.

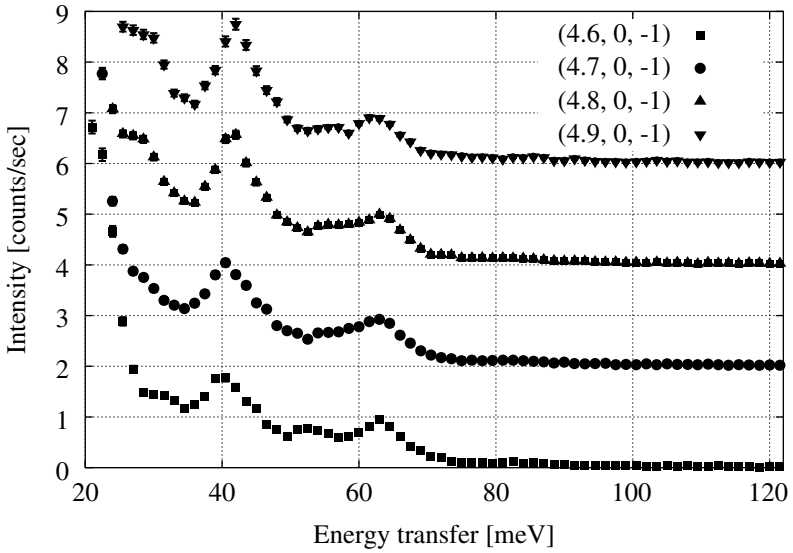

Figure 6. Energy spectra of $YTiO_3$ measured at $q = (4.6, 0, -1.0)$, $(4.7, 0, -1.0)$, $(4.8, 0, -1.0)$ and $(4.9, 0, -1.0)$ at 11 K. The intensity is shown on a linear scale. Each spectrum is offset vertically by 2 for clarity.

A single untwinned crystal was grown by the floating zone method at Hiroshima University. The a-axis was normal to the sample surface, and the a- and c-axis were in the scattering plane. The **Q** positions measured were $(4.6, 0, -1.0)$, $(4.7, 0, -1.0)$, $(4.8, 0, -1.0)$ and $(4.9, 0, -1.0)$. These positions lie between the A point (π, π, π) and the S point $(\pi/2, \pi/2, \pi)$ in the tetragonal Brillouin zone, and a steep dispersion with an intense structure factor is expected at these **Q** positions [35]. We could not access the A point because this corresponds to an allowed Bragg peak and the resulting large background hampered measurement. We note that the longitudinal modes are active and the transverse phonon modes which have components along the c-axis are slightly active in these positions (predominantly a 'longitudinal' geometry). Energy spectra were measured at $T = 50$ and 11 K, above and below T_C, respectively.

We have studied IXS spectra around ∼100 meV (well above phonon energies) in detail in order to detect additional excitations due to orbitons. We have also compared the spectra obtained at two temperatures above and below the ferromagnetic ordering temperature ($T_C \sim 30$ K) in an attempt to detect any change in the orbiton spectrum accompanying the magnetic ordering. Figure 6 shows the energy transfer spectra measured at 11 K, in which several phonon peaks are observed. The phonon peaks around 40 and 60 meV exhibit some small dispersion. In figure 7, we plot the difference between the spectra measured at 11 K and those at 50 K. We were not able to detect any difference between the spectra obtained at these two temperatures. It is worth noting that a recent theoretical study of orbital excitations in the titanates found that the orbital excitations are highly damped modes [37], and therefore would be difficult to observe as a well-defined excitation. Besides, unlike $KCuF_3$, no orbital-order parameter anomaly was detected at the magnetic ordering temperature for $YTiO_3$ [34], suggesting that spin–orbital coupling in this system might be smaller than previously thought.

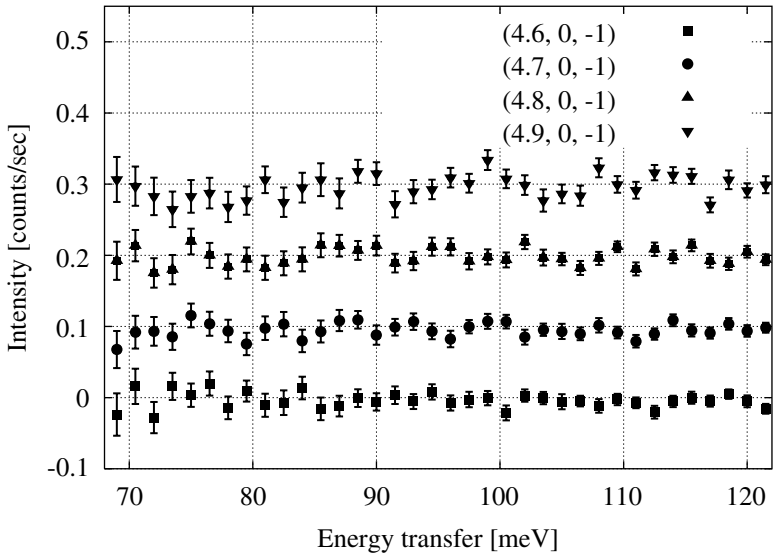

Figure 7. Difference plot of the spectra measured at 50 and 11 K for $YTiO_3$. Each spectrum is offset vertically by 0.1 for clarity.

4. Discussion

There are two possible reasons for the lack of signal observed in these experiments: (1) the cross-section is too small to be observed—either because it is intrinsically very small or because the modes are heavily damped in the **Q** range investigated and thus broadened below detectable levels, or (2) the orbiton energy scale is not within our scan range. In the following, we address each of these possibilities in turn.

In regard to the cross-section, there is presently no theoretical prediction for the size of the orbiton x-ray cross-section. However, the data of figures 3, 5 and 7 can be used to place an experimental estimate on an upper bound to this cross-section for the materials studied. We will express this in terms of the Thomson scattering cross-section for a single electron, for which the differential cross-section/unit solid angle is $\mathrm{d}\sigma/\mathrm{d}\Omega = r_e^2 \cos^2\Theta$ (where $r_e = 2.82 \times 10^{-15}$ m is the classical electron radius and $\cos^2\Theta$ is the usual polarization factor for scattering in the plane of the polarization).

Including the analyser solid angle, the analyser/detector efficiency (a slightly pessimistic ∼50% has been assumed), the photon polarization and the x-ray penetration depth, the expected signal, from a single electron per unit cell, is ∼0.25 cps for $LaMnO_3$, ∼0.5 cps for $KCuF_3$ and ∼0.75 cps for $YTiO_3$ for an incident flux of 2.5×10^{10} cps. The main variation for the different materials comes from the different illuminated sample volumes. For $LaMnO_3$, the error bar (figure 3) in the experimental data set, in the region of 90–200 meV, is approximately $\sigma = 0.005$ cps in a 2 meV bin size. Looking at figure 3, a reasonable upper bound for any signal is about 5σ, suggesting that an energy-integrated signal of ∼0.1 electron/unit cell would be visible if the excitation bandwidth is comparable to, or smaller than, the 6 meV resolution. For the other two materials, for which a temperature difference measurement was possible, stronger statements can be made. In the case of $KCuF_3$, the maximum difference in the spectra at the two temperatures is ∼0.03 cps in the region of 75–120 meV, so that if an orbiton were present in this range, we can state that the change in its signal rate across the magnetic ordering transition

is not more than about 0.1 cps, or ∼0.2 electrons. Similar considerations give an upper bound to any change of 0.06 cps or 0.08 electrons in the region of 70–120 meV for $YTiO_3$. The main contribution for the background intensity originates from the large elastic scattering, the phonon peaks and their tails as a Lorentz function as shown in figure 1. Note that these limits appropriate for the particular Brillouin zones where the measurements were carried out and, for a proper comparison to theory, the detailed structure factor should be calculated in those zones.

Turning now to the second possibility, namely that the energy scale of the orbiton is out of the range of the present experiment, we first note that there is considerable support for an orbital excitation in the range of 100–200 meV, see e.g. [14, 38]. However, a number of authors have suggested that the orbiton mode would be significantly higher, perhaps as high as 2 eV. For example, *ab initio* quantum chemistry calculations put the splitting between e_g orbitals $\Delta_{JT} = 1.2$ eV in $LaMnO_3$, optical conductivity measurements show gaps of the order of 1 eV which have been interpreted as arising from d–d excitations (see e.g. [39, 40]) and model calculations, based on Hamiltonians with JT and electron–phonon coupling terms predict orbital excitations ('polaronic absorption') at $\Delta_{JT}/2$ [13, 41]. Indeed, resonant Raman scattering experiments claim to have observed such features [18]. Finally, two recent experiments utilizing ellipsometry [42] and resonant IXS [43] both saw temperature dependence in the excitation spectra at energies around 2 eV. This temperature dependence was argued to be associated with intersite d–d excitations. The bare energy scale for such excitations is the on-site JT splitting. If this is indeed of the order of 2 eV and these interpretations are correct, then it is likely that any collective orbital excitations would also be on this kind of scale and hence unobservable in the present experiment.

5. Conclusion

We have carried out high-resolution IXS experiments in $LaMnO_3$, $KCuF_3$ and $YTiO_3$ to search for orbiton modes. Such modes had previously been identified using Raman scattering in $LaMnO_3$, although this interpretation has been controversial. IXS offers some advantages in this endeavour, including the ability to measure the momentum dependence of any excitation observed. However, no such scattering was observed in these experiments. It is not possible to say from the present experiments alone whether this is because the orbitons are at a much higher energy scale, as some authors have argued, or because the orbiton x-ray cross-section is too small to be observed. We have provided upper bounds on the cross-section for orbitons in several samples over selected ranges of energy and momentum transfer. We hope that these will provide impetus for theorists to provide more precise information about these excitations. Given such information, the search region might be narrowed and, if the sample elastic scattering were reduced (for example, with careful surface preparation), it might be possible to improve our sensitivity by as much as one order of magnitude. Going further, in our opinion, would require a different sort of experiment—possibly sacrificing energy resolution for increased count rate, something that would be especially favourable if the orbiton energy were ∼eV.

Acknowledgments

We thank S Okamoto, S Ishihara, and V Perebeinos for helpful discussions. We also thank G Shirane for the loan of the $KCuF_3$ crystal. ST acknowledges financial support

from the Ministry of Education, Science, Sports and Culture (Grant-in-Aid for Young Scientists). The experiments were performed under the SPring-8 proposals 2002A0562, 2003A0683 and 2003B0019. The work at Brookhaven (National Laboratory) was supported by the US Department of Energy, Division of Materials Science, under contract No. DE-AC02-98CH10886.

References

[1] Goodenough J B 1955 *Phys. Rev.* **100** 564
[2] Kanamori J 1959 *J. Phys. Chem. Solids* **10** 87
[3] Kugel K I and Khomskii D I 1972 *JETP Lett.* **15** 446
Kugel K I and Khomskii D I 1973 *Sov. Phys.—JETP* **37** 725
[4] Kiryukhin V *et al* 2003 *Phys. Rev.* B **67** 064421
[5] Khaliullin G and Maekawa S 2000 *Phys. Rev. Lett.* **85** 3950
[6] Murakami Y *et al* 1998 *Phys. Rev. Lett.* **81** 582
[7] Rodoríguez-Carvajal J *et al* 1998 *Phys. Rev.* B **57** R3189
[8] Wilkins K S B *et al* 2003 *Phys. Rev. Lett.* **91** 167205
[9] Thomas K J *et al* 2004 *Phys. Rev. Lett.* **92** 237204
[10] Dhesi S S *et al* 2004 *Phys. Rev. Lett.* **92** 056403
[11] Ishihara S, Inoue J and Maekawa S 1997 *Phys. Rev.* B **55** 8280
[12] Saitoh E *et al* 2001 *Nature* **410** 180
[13] Allen P B and Perebeinos V 1999 *Phys. Rev. Lett.* **83** 4828
[14] van den Brink J 2001 *Phys. Rev. Lett.* **87** 217202
[15] Grüninger M *et al* 2001 *Nature* **418** 39
[16] Saitoh E *et al* 2001 *Nature* **418** 40
[17] Martín-Carrón L and de Andrés A 2004 *Phys. Rev. Lett.* **92** 175501
[18] Krüger R *et al* 2004 *Phys. Rev. Lett.* **92** 097203
[19] Baron A Q R *et al* 2000 *J. Phys. Chem. Solids* **61** 461
[20] Wollan E O and Koehler W C 1955 *Phys. Rev.* **100** 545
[21] Ishihara S *et al* 2004, private communication
[22] Martín-Carrón L *et al* 2002 *Phys. Rev.* B **66** 174303
[23] Okazaki A and Suemune Y 1961 *J. Phys. Soc. Japan* **16** 671
[24] Hutchings M T *et al* 1969 *Phys. Rev.* **188** 919
[25] Hirakawa K and Kurogi Y 1970 *Prog. Theor. Phys.* **S46** 147
[26] Satija S K *et al* 1980 *Phys. Rev.* B **21** 2001
[27] Paolasini L *et al* 2002 *Phys. Rev. Lett.* **88** 106403
Caciuffo R *et al* 2002 *Phys. Rev.* B **65** 174425
[28] Oles A M *et al* 2000 *Phys. Rev.* B **61** 6257
[29] Ueda T 1991 *Solid State Commun.* **80** 801
[30] Ulrich D C *et al* 2002 *Phys. Rev. Lett.* **89** 167202
[31] Hester J R *et al* 1997 *Acta Crystallogr.* B **53** 739
[32] Akimitsu J *et al* 2001 *J. Phys. Soc. Japan* **70** 3475
[33] Itoh M *et al* 1999 *J. Phys. Soc. Japan* **68** 2783
[34] Nakao H *et al* 2002 *Phys. Rev.* B **66** 184419
[35] Khaliullin G and Okamoto S 2002 *Phys. Rev. Lett.* **89** 167201
Khaliullin G and Okamoto S 2003 *Phys. Rev.* B **68** 205109
[36] Ishihara S 2004 *Phys. Rev.* B **69** 075118
[37] Kikoin K *et al* 2003 *Phys. Rev.* B **67** 214418
[38] van den Brink J *et al* 1998 *Phys. Rev.* B **58** 10276

[39] Jung J H *et al* 1997 *Phys. Rev.* B **55** 15489
[40] Jung J H *et al* 1998 *Phys. Rev.* B **57** 11043
[41] Perebeinos V and Allen P B 2001 *Phys. Rev.* B **64** 085118
[42] Kovaleva N N *et al* 2004 *Preprint* cond-mat/0405509
[43] Grenier S *et al* 2004 *Preprint* cond-mat/0407326